

AN ASSESSMENT OF MININEC AND ITS USE IN THE TEACHING OF ANTENNA THEORY

B.A. AUSTIN

Department of Electrical Engineering and Electronics,

University of Liverpool,

P.O. Box 147, Liverpool, L69 3BX,

United Kingdom.

ABSTRACT

MININEC is a compact, Method of Moments code, written specifically for the personal computer which has evolved considerably in the last decade. This paper presents an assessment of the program and discusses its use in the teaching of antenna theory to undergraduates. The results of a number of validation exercises on the code are included and the simulation of loaded wire antennas, using MININEC, is discussed.

1. INTRODUCTION

Computational Electromagnetics (CEM) has made enormous progress in the last decade. Whereas the use of mainframe and even super-computers is now common-place for the solution of very large problems in reasonable periods of time [1] the application of such techniques as the Method of Moments (MM) on the ubiquitous personal computer has not lagged behind. This has been made possible in the field of wire antenna analysis by the availability and subsequent development of the MININEC software [2]. Described by its originators as a compact code suitable for use on a microcomputer and applicable to small problems, MININEC has now established itself as an extremely useful adjunct in the teaching of antenna theory and as a research tool in its own right.

MININEC, when first made available in 1982 and for some while thereafter, was viewed by many electromagneticists as something of a novelty not to be taken too seriously and certainly not to be trusted. A probable reason for these views was the fact that its public domain status meant that it proliferated through sections of the antenna community (both professional and radio amateur) at such a rate that the excellent documentation supplied by its originators [2] was often lost on the way! The code was frequently misused and its capabilities and limitations certainly misunderstood. It is the intention in this paper to review the MININEC program in its evolutionary forms; to provide some examples to validate its performance and to show how it has been used most effectively in the undergraduate teaching environment.

2. BACKGROUND

MININEC was written in the BASIC language and uses a modified Galerkin procedure to solve the electric field integral equation (EFIE) for the current distribution along a thin-wire, or series of suitably interconnected such wires for given source and loading configurations. Being compact, the original MININEC ran to only 550 lines of code and fitted within the 64 kilobyte memory capability of the pre-"pc" era of microcomputers. As such, it was only capable of handling 40 unknowns [2] and this set the original limit as regards the number of wires used, their segmentation and the number of discrete sources and loads which could be accommodated. Subsequently, up to 10 wires, divided into a total of 70 segments, could be handled with the resulting structure being either in free space or above an infinite, perfect ground plane.

Various extensions, modifications and up-grades to MININEC followed rapidly [3-6], mainly from the code's originators but also from others [4], who added a graphics capability for displaying the geometry of the modelled structure as well as radiation patterns and input impedance plots on a Smith

chart. The fundamental limitation on the size of problem that could be handled is the BASIC compiler common to personal computers and this set 100 unknowns as the typical upper limit. However recently available compilers have allowed this limit to increase to about 200 unknowns in version 3, with the principle limitation now being set by the size of the CPU [7]. The latest versions of MININEC [6], of which two more, MN and ELNEC, have appeared most recently within the amateur radio literature [8], are available as sophisticated, well-structured and user-friendly programs which are based on MININEC version 3. As such, they represent a significant advance over their predecessors by incorporating excellent graphics with the capability of viewing the geometrical configurations in three dimensions and, in some cases even allowing them to be rotated for viewing from any angle. Antenna currents can be plotted on the wires in magnitude and phase formats and far-field azimuth and elevation patterns in polar or rectangular coordinates. In addition, the patterns produced by two antennas can be compared easily at a keystroke.

Validation of the computed results produced by any analytical software is obligatory before the code can be used with confidence. More will be said about this later but, at this stage, it should be made clear what the essential differences are between MININEC and NEC, the Moment Method code from which it was originally derived. NEC, [9], with its version 3 the most recently available, has become regarded as the virtual industry-standard for the analysis of so-called low-frequency antennas [10]. Computed results obtained from NEC are therefore used frequently as the standard against which those obtained from other techniques, such as MININEC, are judged. This may seem strange given the apparent lineal descendancy of MININEC from NEC. However there are significant differences between them. Firstly, NEC solves the EFIE or the magnetic field integral equation (MFIE) by using either wire elements or surface patches to configure the geometry in question. MININEC

is based on the numerical solution of the EFIE using thin wire elements. Both codes of course use the Method of Moments to do this but NEC uses a three-term (constant, sine and cosine) form as the current basis function with a delta function as the weighting function. By contrast, MININEC uses the Galerkin procedure, with pulse basis and testing functions and this, for some applications, has real advantages because of the resulting symmetrical impedance matrix [11, 12]. Essentially therefore MININEC and NEC are different formulations and it is therefore valid to use the results from one to check or confirm those from the other, assuming appropriate use of each for the problem in hand.

From here on only the most recent versions of MININEC [5-8] will be considered. These now offer the capability of computing both near and far-fields and also include real ground as well as free space and perfect ground planes. However, unlike NEC, only far-field characteristics are computed over real ground. The current distribution and driving point impedance are determined over perfect ground. This can lead to erroneous results with certain antenna configurations particularly if they are close-to or fed against ground. Up to ten concentric ground zones may be specified [8] or up to five zones with linear boundaries [5]. The conductivity and relative permittivity of each zone are defined by the user and these zones may also be at different heights above the xy (horizontal) plane, thus effectively simulating the topography of the land. The first zone can also accommodate a radial wire ground screen. Again, there are differences between how MININEC and NEC handle these far field cases. MININEC uses the Fresnel reflection coefficient method whereas NEC also has the capability of using the considerably more complex and more realistic Sommerfeld integral method for computing the effects of ground reflections as well as for determining the driving-point impedance over real ground as well as for wires both very close to and even penetrating the air-ground interface.

The choice of segmentation schemes is a key aspect for the successful use of both NEC and MININEC. The various versions of the MININEC documentation [2, 5, 6] contained detailed information on the most appropriate segmentation schemes for antennas and structures which were either electrically short, resonant or anti-resonant. Adherence to these recommendations generally produced accurate results for simple antennas which contained straight elements and which did not require the inclusion of imbedded transmission lines, such as the log periodic dipole array (LPDA). However, junctions between wires with significantly different lengths could produce completely erroneous results unless careful attention was paid to the ratio of segment lengths on interconnected wires [13]. The use of a tapered segmentation scheme is recommended to overcome this problem since it also minimises the total number of segments used and thereby reduces the run-time. Automatic segmentation routines, which can, if required, be overridden by the user, are now provided in the latest versions of code, such as MN. These also automatically taper the segments in the vicinity of junctions should this be necessary.

Where MININEC is used to model geometries containing bent wires such that the included angle between wires is less than 180 degrees, then errors can result unless suitable precautions are taken. These errors occur as frequency offsets, with the computed results being displaced upwards in frequency by as much as 3 or 4 per cent when compared with those generated by NEC. This frequency offset effect also occurs when the radius of the elements is increased. Thus thick or fat structures must be modelled with care unless the code used has a built-in correction for these effects. The MN version of the code, due to Beezley [8], does contain improved algorithms which correct for all these offsets due to either the use of thick wires, the geometric distortion at bent-wire junctions and for discontinuities in segment lengths.

3. VALIDATION OF MININEC

Regardless of its application and its degree of sophistication a piece of simulation software is of no value whatsoever if the results it produces are incorrect. This is equally true whether the program is used in research, development or in the educational process. MININEC therefore has been subjected to considerable assessment over the years in order to validate the results for a variety of antenna configurations [8, 14]. Some of these, from this latter validation exercise, will be discussed here.

a) Input impedance of a halfwave dipole

It is recognized [15] that the input impedance of an antenna is the parameter most sensitive to computational error because of its critical dependence on the current distribution. In addition the specific geometrical details of the feed region are especially important in determining input impedance. Whereas NEC allows for a variety of different source schemes, MININEC only accommodates a simple voltage source at specified points on a wire. The most recent versions of the code also allow current sources to be used. Other than the segment tapering discussed above no special geometrical factors are considered in the feed region. Figure 1 shows computed values of the input impedance of a dipole antenna of length $2h = 0.5$ m, radius, $a = 0.001$ m at 300 MHz. Results for this geometry are shown using MININEC, NEC version 2, a code due to Richmond [16] and, from a Galerkin-based code with a tapered segmentation scheme [17] for five specific feed region geometries. Also plotted (though unrelated to the number of segments) is the result from King and Harrison [18], by way of comparison. Note that both the NEC and Richmond results agree with those of King when about 5 segments per quarter wavelength were used. MININEC required somewhat more, with the reactance being the more critical parameter. The data from [17] seem to converge to those of King, in the real part, for a segment count between those of NEC and MININEC. By contrast, the reactive components from [17]

show no evidence, from the data available, of converging on King's value. One is left to conclude that MININEC computes input impedance at least as accurately as do other well respected procedures but that the true value of the input impedance of the half wave dipole remains an interesting, though as yet, uncertain quantity, particularly when the detailed shape of the feed region is considered.

b) V-dipole antenna

The centre-fed V-dipole antenna illustrates the problem of modelling bent wire antennas. Figure 2 shows the input impedance of such an antenna where $2h = 0.5\lambda$ and of wire radius a , for the case where $h/a = 2 \times 10^4$ [19]. This result was obtained from a Galerkin procedure using sinusoidal expansion and testing functions which agrees with the so-called King-Middleton second order solution [18]. Also shown are the MININEC results, using [6] and those from NEC for the input impedance. The real part, as given by both codes, is in excellent agreement for all values of the included angle θ whereas the MININEC imaginary part deviates markedly as θ is decreased. Doubling the number of segments per wire from 10 to 20 produced no change in the real part in either code and only corrected the imaginary component from MININEC by about 20 percent when the included angle was 30 degrees. By contrast the NEC2 results agree very well with those of Jones [19]. However if a tapered segmentation scheme is used in the vicinity of the source then the MININEC results are indistinguishable when plotted with those computed with NEC.

c) Yagi-Uda array

This antenna, which dominates most of our skylines, has been subjected to considerable analysis, measurement and optimization. A two element array, from [20] was used as the basis for comparison of computed results of input impedance, gain and front-to-back ratio. The array consisted of a driven element of length 0.470λ and a reflector of 0.494λ , spaced 0.141λ apart

and both elements were untapered with radii of 0.0006λ . Good agreement was found between results from [20], those using MININEC [6] and a moment method code developed by Pozar [21] specifically for modelling simple Yagi arrays. Only the front-to-back ratio is shown here in Figure 3 because it illustrates the degree of agreement between three very different computational techniques for determining a parameter which is particularly sensitive to the current distribution on the array. Lawson assumed it to be sinusoidal while Pozar used a piece-wise sinusoidal expansion function in a Galerkin procedure. Both agree well with the MININEC result at the F/B peak and continue to do so across the frequency range. The sinusoidal distribution produces excellent agreement at the peak but some deviation at the other frequencies. Frequently, the experimental results obtained by Viezbicke [22] are quoted as the standard reference when assessing the Yagi-Uda antenna. Figure 4 shows the effect on gain of changing the spacing between the 0.482λ elements of a two element array where the parasitic is a reflector. Whereas the data from MININEC, NEC, Lawson and Pozar are in close agreement, those of Viezbicke deviate markedly and indicate very little dependence on spacing. This conflicts with practical experience and with the results of an detailed analysis [24] of this antenna.

d) **Loaded short monopole**

Hansen [23] has shown how the radiation efficiency of an inductively loaded short monopole varies with the position of the appropriate inductor required to produce resonance. Since all versions of MININEC allow the inclusion of lumped RLC loads within a structure, at defined segments, the antenna in Figure 5 was modelled. Here $h = 1 \text{ m}$ and Q_L is the quality factor of the inductor. There is excellent agreement between Hansen's results and those from MININEC. It was this ability of the code to accurately predict such characteristics for antennas of this type which led to the development of a simulation exercise for use by undergraduates which will be described

next.

Numerous other validation exercises have been performed [14] to assess the accuracy of the results predicted by MININEC. As indicated here it was found that the code produces entirely acceptable results for a variety of wire antenna configurations, both single-element and arrays, and when loaded with lumped components.

4. A TEACHING EXERCISE

The difficulty of mounting meaningful antenna experiments in a teaching laboratory environment, other than for demonstration purposes, is well known. Prior to the availability of readily accessible, user-friendly computer programs like MININEC (particularly in its most recent versions), courses on antennas tended to be entirely theoretical with occasional use being made of a microwave test-bench to examine characteristics like the radiation patterns of a rather limited number of antennas.

Whereas such practical experience is still to be encouraged there is now considerable scope to go well beyond what is possible in that rather limited situation. A computer modelling exercise using MININEC version 3 will now be described. It has been run very successfully since 1986 at the Universities of the Witwatersrand, in Johannesburg, and Liverpool [25].

a) A thin-wire short dipole

The characteristics of a thin-wire, short dipole ($2h \ll \lambda$) in free space are readily calculable using some fairly simple, through appropriate, approximations. It is assumed that the current distribution along the centre-fed antenna is triangular by choosing its length, $2h < \lambda/4$.

Therefore, on this basis, the radiation resistance may be written as:

$$R_{\text{rad}} = 20 \pi^2 \left(\frac{2h}{\lambda} \right)^2 \quad (1)$$

while its input reactance can be obtained approximately by treating the antenna as an opened out, open-circuit transmission line, if one assumes that this cylindrical antenna is the limiting case of a biconical antenna with cone half-angle θ . Incidentally, as Collin [26] points out, the current on such an infinitely thin cone becomes a pure sinusoidal standing wave, which provides the basis for the well-used assumption of a sinusoidal current distribution on thin-wire antennas. Based on Collin's approach we proceed as follows:-

The characteristic impedance of the biconical structure is given by:

$$Z_o = 120 \ln \cot \frac{\theta}{2} \quad (2)$$

Now, the cylindrical antenna in Figure 6 is equivalent to a transmission line whose characteristic impedance varies gradually along its length. For θ small we have that $\tan \theta = a/x \approx \theta$, therefore:

$$\cot \frac{\theta}{2} \approx 2/\theta = 2x/a \quad (3)$$

Hence the characteristic impedance of the thin cylindrical antenna at the point x is:

$$Z_o(x) \approx 120 \ln \frac{2x}{a} \quad (4)$$

and so, to a first approximation, the average value of Z_o for an antenna of length $2h$ is given by:

$$Z_o = \frac{120}{h} \int_0^h \ln \frac{2x}{a} dx = 120 \left[\ln \frac{h}{a} - 1 \right] \quad (5)$$

The input reactance, X_{IN} , of this thin-wire antenna is then obtained from the lossless transmission line model with the load, Z_L , being open-circuit, hence $Z_L \rightarrow \infty$.

$$\text{Thus } X_{IN} = \frac{Z_o (Z_L + j Z_o \tan kh)}{Z_o + j Z_L \tan kh} \quad (6)$$

$$\text{or } X_{IN} = -j Z_o \cot kh \quad (7)$$

where $k = 2\pi/\lambda$.

The theoretical input impedance of this short, thin-wire dipole is therefore:

$$Z_{IN} = 20 \pi^2 \left(\frac{2h}{\lambda} \right)^2 - j Z_o \cot kh \quad (8)$$

where the only losses are assumed to be due to radiation.

For the simulation exercise a centre-fed dipole of length $2h = 5$ m and of radius $a = 2$ mm was used at a frequency of 10 MHz. From (5) $Z_o = 819 \Omega$ and therefore, from (8), the input impedance is readily calculated as $Z_{IN} = 5.48 - j1418 \Omega$. Whereas the effort in obtaining this result is minimal the learning process is considerably reinforced when the same antenna is analysed using MININEC. Before doing so, two constraints must be satisfied: that $a/\lambda \ll 1$ and that $2h/a \gg 1$. These imply effectively that only axial currents flow on the conductor. Clearly, in this case, both are satisfied. The choice of segmentation scheme is determined by a number of factors, with increased accuracy resulting from an increase in segments, N , into which the wire is divided as long as a further constraint, that $\Delta/a > 10$, is not violated, where Δ is the length of a segment. However, increasing the number of segments also means an increase in computation time and so a sensible choice of N would be based on the recommendations in [2]. Choosing $N = 8$

produces the computed input impedance $Z_{IN} = 5.48 - j1284 \Omega$.

The agreement for the resistive components is exact. Thus the postulated triangular current distribution is confirmed and may be plotted, as further evidence, by examining the current distribution pulse-by-pulse in the appropriate MININEC file.

The computed value of input reactance and that from the transmission line model agree to within about 10 percent. This is a reasonable engineering result and indicates the adequacy of the simple transmission line model in this case.

b) **An inductively loaded short dipole**

By inserting a lumped inductor with $X_L = j1248 \Omega$ at the feed point the antenna is made to resonate. Realistically, that inductor will have finite Q where

$$Q = 2\pi fL/R \quad (9)$$

with R being the loss resistance of the coil.

Using $Q = 100$, which is a reasonable value for an air-cored inductor suitable for this application, yields $R = 12.84 \Omega$ and therefore the input resistance of the antenna rises to $R_{IN} = 5.48 + 12.84 = 18.32 \Omega$. By inserting this inductive load at the source in the MININEC model the computed input impedance becomes $Z_{IN} = 18.3 - j0.19 \Omega$; effectively resonant, as intended.

Clearly the loss introduced by this loading inductor decreases the radiation efficiency, η , where

$$\eta = R_{rad} / (R_{rad} + R_{loss}) \quad (10)$$

$$\text{thus } \eta = \frac{5.48}{18.32} \times 100 = 29.9 \text{ percent}$$

In addition, the gain, G, will be reduced because

$$G = \eta D \quad (11)$$

where D is the directivity of the antenna.

A reasonable assumption for the student to make is that the directivity of the unloaded antenna is 1.5 since it is electrically short. The MININEC simulation effectively confirms this by yielding $D = 1.79$ dBi (1.51). When the antenna is loaded with that inductor, the computed gain is -3.46 dBi (0.45).

$$\text{Thus } \eta = \frac{0.45}{1.51} \times 100 = 29.9 \text{ percent, exactly as calculated above.}$$

Increased radiation efficiency (and hence gain) can be achieved by moving the inductive loading out along the arms of the antenna, as shown previously by Hansen [23]. Again, this case is readily calculable by hand using Collin's [26] transmission line approach and is illustrated in Figure 7.

If two, equal, inductors are moved a distance ℓ from the centre of the antenna and their value adjusted to maintain resonance at the feed point, then it can be shown that the inductance required per arm of the antenna is:

$$L_{\text{per arm}} = \frac{Z_0}{4 \pi f} (\cot k (h - \ell) - \tan k\ell) \quad (12)$$

This result follows from the transmission line approximation of the antenna where, again, the input reactance at the feed point is given by:

$$X_{\text{IN}} = \frac{Z_0 (X_L' + j Z_0 \tan k\ell)}{Z_0 + j X_L' \tan k\ell} \quad (13)$$

with Z_0 from (4) and X_L' is the load on the equivalent transmission line of length ℓ , which consists of two inductors of $L/2$ in series with an open-circuit transmission line of length $(h-\ell)$.

$$\text{Thus } X_L' = j\omega L - j Z_0 \cot k (h-\ell) \quad (14)$$

At resonance the numerator of (13) must be zero, therefore:

$$Z_o (\cot k (h-l) - \tan k\ell) = \omega L \quad (15)$$

from which (12) follows easily since the required inductance per arm is simply $L/2$.

If these inductors are placed centrally within each arm of the antenna then $\ell = h/2 = 1.25$ m and so, from (12), $L_{\text{per arm}} = 22.6 \mu\text{H}$ or a lumped reactance of 1419Ω per arm.

After inserting these inductive reactances (initially with $Q \rightarrow \infty$) at the mid-point of each arm (segments 3 and 9) in the MININEC model the computed input impedance is $Z_{\text{IN}} = 15.83 + j454$. Clearly the antenna is not resonant. Some iteration is required as the inductive loads are reduced. After one or two judicious changes to a value of $L_{\text{per arm}}$ of $19.7 \mu\text{H}$ resulted in an input impedance of $12.56 + j0.17$ which is essentially resonant. It should be noted that the simple transmission line model produced a value for the inductive loads which was about 13 percent lower than that obtained from the simple model. Again, this indicates the usefulness of a simple procedure which is based on a plausible model.

c) Current distribution along the loaded antenna

Considerable insight may be gained into the characteristics of this off-centre loaded antenna by examining its current distribution. Firstly, the effect of the inductors is to maintain the current approximately constant between the feed point and each load; secondly, the boundary condition at the end of each wire requires that the current there is zero and thirdly, because $(h-l) \ll \lambda/4$, the current decays linearly from each inductor to the wire-end. This argument therefore suggests that the current distribution along this particular loaded antenna will be trapezoidal. Of course MININEC displays the current at each segment and therefore this postulated distribution is easily confirmed and is shown in Figure 8.

It will be noted that the MININEC distribution shows some current peaking at the position of the loads. This effect was discussed by Hansen

[23] and is caused by the fact that the inductance required to force resonance in the antenna is actually slightly larger than that required to maintain the current constant between source and load. The additional inductive element manifests itself by a slight increase in current amplitude at each load. Such agreement between MININEC and the literature is most reassuring, not only to the student!

By effectively causing the current to maintain its value as far as the load, instead of falling linearly to zero, as with the unloaded antenna, the current moment, and with it the radiation resistance, of the antenna have been increased. Current moment is simply related to the area A under the current distribution curve, which in turn is a measure of the field intensity (E or H) produced in the far-field by the antenna. Thus, for the unloaded antenna, with a triangular current distribution with maximum value, I, :

$$A_1 = I h \quad (16)$$

The loaded antenna, with the trapezoidal current distribution of the same peak value, has a current moment of:

$$A_2 = (h \times I) + 2 \left(\frac{h}{4} \times I \right) = \frac{3 h I}{2} \quad (17)$$

Now the power radiated by the antenna is:

$$P \propto \frac{E^2}{Z_i} \propto H^2 Z_i \quad (18)$$

where $Z_i \approx 120 \pi \Omega$ is the intrinsic impedance of free space. Clearly, therefore, the ratio between the powers radiated by the loaded and unloaded antennas is:-

$$P_2/P_1 = (A_2/A_1)^2 = (3/2)^2 = 2.25 \quad (19)$$

If the peak feed-point current into each antenna is the same then the increase in radiated power must be due to an increase in radiation resistance

in the loaded antenna compared with that of its unloaded counterpart. Thus:

$$\frac{R_{\text{loaded}}}{R_{\text{unloaded}}} = 2.25 \quad (20)$$

By comparison, the two values of R_{rad} computed by MININEC for these loaded and unloaded antennas were 12.56 Ω and 5.48 Ω respectively. Their ratio is 2.29 - in excellent agreement with (20).

Finally, the improvement in radiation efficiency which was achieved by displacing the loading from the centre feed-point is readily calculable and checked by using MININEC. Again we use a realistic value of $Q = 100$ for the loading inductors. From the value of 19.7 μH required for resonance we calculate the loss resistance (ignoring any losses in the actual antenna conductor) as $X_L/Q = 12.38 \Omega$. However this value is transformed by the section of the antenna between the feed-point and the load such that the real part of the input impedance, as determined by MININEC, is 38.6 Ω . This corresponds to the sum of R_{rad} plus R_{loss} . The radiation resistance alone is found easily, with MININEC, if one assumes that the inductors are lossless (i.e. $Q \rightarrow \infty$). Hence, the code yields $R_{\text{IN}} = R_{\text{rad}} = 12.6 \Omega$, from which the radiation efficiency follows as $\eta = \frac{12.6 \times 100}{38.6} = 32.6$ percent

As was done before the radiation efficiency can also be obtained by computing G and D and then using (11). Thus, with lossless inductors $G - D = 1.80$ dBi (1.514) while when $Q = 100$, $G = -3.07$ dBi (0.493). Therefore the radiation efficiency, from (11) is $\eta = G/D = 32.6$ percent, as expected.

The effect of moving the loading inductors away from the feed-point has increased the radiation efficiency from 29.9 percent to 32.6 percent, which, seemingly, is not too significant. However it should be noted that this change was accompanied by an increase in input resistance from 18 to 39 Ω which eases the impedance matching requirements quite considerably if the

antenna is to be fed with 50Ω coaxial cable. This inter-relationship between VSWR and radiation efficiency occurs frequently when attempts are made to enhance the performance of simple antennas, usually by some form of loading to increase their VSWR-bandwidth. It therefore emphasises the need to always consider both aspects when evaluating such antennas.

5. CONCLUSIONS

The evolution of MININEC has been reviewed from its release a decade ago as a very simple wire modelling code to its present status where both its capabilities and its usefulness have been enhanced considerably. Its role in the teaching of aspects of antenna theory has been used to illustrate some of its features and various examples were included of validation exercises which were designed to determine the accuracy of the code in predicting the performance of wire antennas.

It is concluded that the most recent versions of MININEC, (version 3 onwards), are accurate and highly versatile codes, which are particularly simple to use. The advanced graphics features now available make them ideal for use in antenna simulation exercises in the teaching environment.

REFERENCES

- [1] E.K. Miller, "A selective survey of computational electromagnetics", IEEE Trans. Antennas Propagat., Vol.AP-36, pp.1281-1305, 1988.
- [2] A.J. Julian, J.C. Logan and J.W. Rockway, MININEC: A mini-numerical electromagnetics code, TD516, Naval Ocean Systems Centre, San Diego, CA, 1982.
- [3] S.T. Li, J.C. Logan, J.W. Rockway and D.W.S. Tam, "Microcomputer Tools for Communications Engineering", Artech House, 1984.

- [4] D.A. MacNamara and L. Botha, MININEC Ver.1.2, Council for Scientific and Industrial Research, Pretoria, 1985.
- [5] J.C. Logan and J.W. Rockway, The New MININEC (Version 3): A Mini-Numerical Electromagnetics Code, TD938, Naval Ocean Systems Centre, San Diego, CA, 1986.
- [6] J.W. Rockway, J.C. Logan, D.W.S. Tam and S.T. Li, The MININEC System: Microcomputer Analysis of Wire Antennas, Artech House, 1988.
- [7] J.C. Logan and J.W. Rockway, "The evolution of MININEC" IEEE International Symposium on EMC, Seattle, 66-68, 1988.
- [8] R. Lewallen, "MININEC: The other edge of the sword", QST, Vol.75 (2), pp.18-22, 1991.
- [9] G.J. Burke and A.J. Poggio, Numerical Electromagnetics Code (NEC) - Method of Moments Parts I, II and III, NOSC TD116, Naval Ocean Systems Centre, San Diego, CA, 1980.
- [10] E.K. Miller and G.J. Burke, "Low-frequency computational electromagnetics for antenna analysis, "Proc. IEEE, Vol.80, pp.24-43, 1992.
- [11] J. Moore and R. Pizer, Moment Methods in Electromagnetics, Research Studies Press, 1984.
- [12] B.A. Austin and K.P. Murray, "The generation of antenna characteristic modes from the impedance matrix using the moment method", IEE 7th Intl. Conf. Antennas Propagat., Publ.No.333, 713-716, 1991.
- [13] S.J. Kubina, "Numerical modelling methods for predicting antenna performance on aircraft", AGARD Lecture Series, No.131, 9.1-9.38, 1983.
- [14] B.A. Austin, "Validation of microcomputer antenna codes", IEE 6th Intl. Conf. Antennas Propagat., Publ.No.301, 427-431, 1989.
- [15] Popovic, B.D., CAD of Wire Antennas and Related Radiating Structures, Research Studies Press Ltd., Taunton, England, 1991.

- [16] J.H. Richmond, Computer program for thin-wire structures in a homogenous conducting medium, NASA Contract Report, CR-2399, June 1974.
- [17] D.J.J. Janse van Rensburg and D.A. McNamara, "On quasi-static source models for wire dipole antennas", Microwave and Optical Technology Letters, Vol.3, pp.396-398, 1990.
- [18] R.W.P. King and C.W. Harrison, Antennas and Waves, Appx.4, The MIT Press, Cambridge, Mass., 1969.
- [19] J.E. Jones, "Analysis of the symmetric centre-fed V-dipole antenna", IEEE Trans. Antennas Propagat. Vol.AP-24, pp.316-322, 1976.
- [20] J.L. Lawson, Yagi Antenna Design, American Radio Relay League, Newington, 1986.
- [21] D.M. Pozar, Antenna Design using Personal Computers, Artech House Inc. Mass., 1985.
- [22] P. Viezbicke, Yagi Antenna Design, NBS Technical Note 688, US Dept. of Commerce, 1976.
- [23] R.C. Hansen, "Optimum inductive loading of short whip antennas", IEEE Trans. Vehicular Techn., Vol.VT-24, pp.21-29, 1975.
- [24] D.K. Cheng and C.A. Chen, "Optimum element spacing for Yagi-Uda arrays", IEEE Trans. Antennas Propagat., Vol.AP-21, pp.615-623, 1973.
- [25] B.A. Austin, "A simulation exercise in antenna analysis using MININEC", Int. J. Elect. Enging. Educ., Vol.26, pp.355-365, 1989.
- [26] R.E. Collin, Antennas and Radiowave Propagation, McGraw-Hill, New York, 1985.

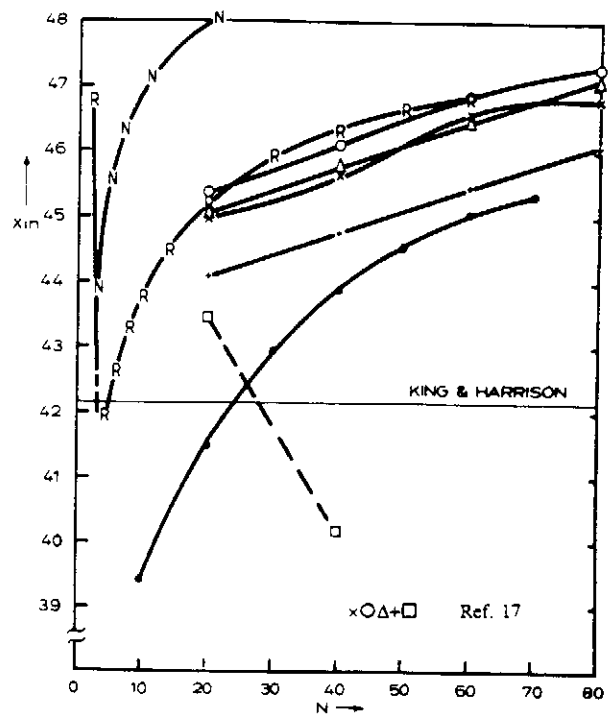
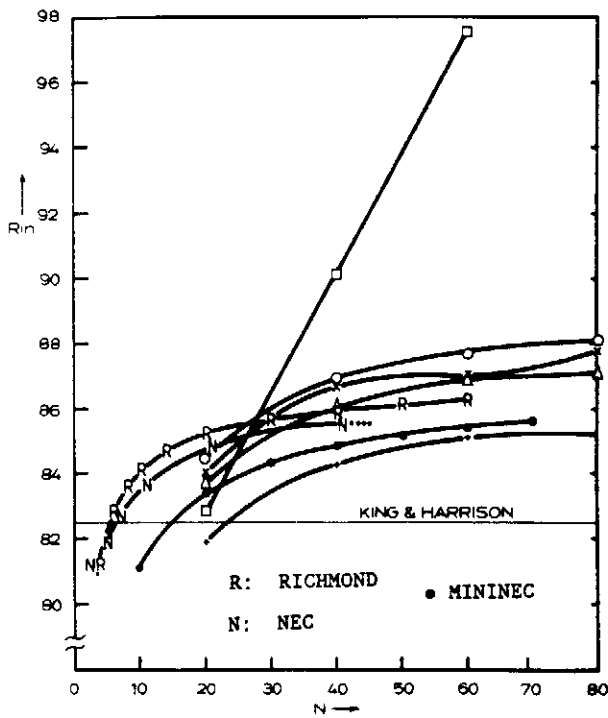


Fig.1. Computed input impedance of the half wave-dipole. ($2h = 0.5m$; $a = 1mm$; $f = 300MHz$).

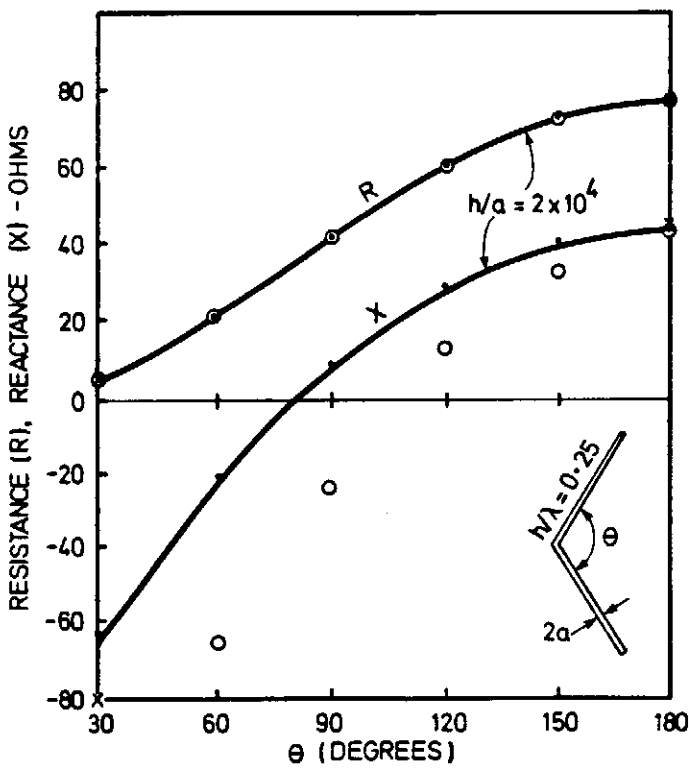


Fig.2. Input impedance of half-wave V antenna; — ref.19; O MININEC (no taper); • NEC

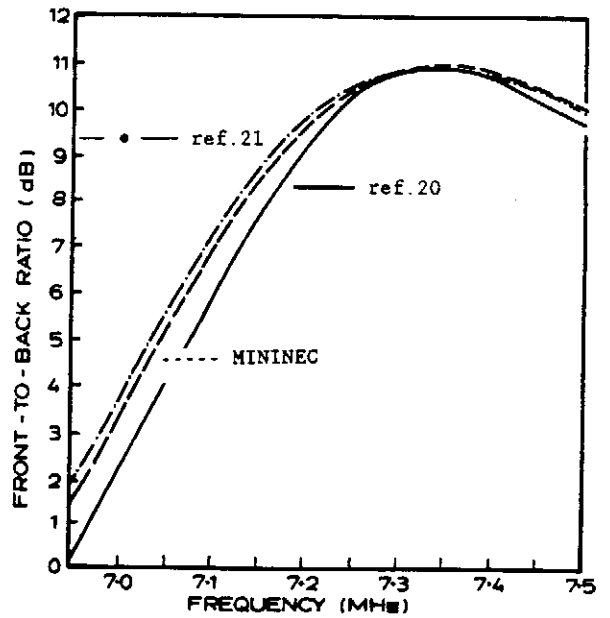


Fig.3. Computed front-to-back ratio of Yagi-Uda array;

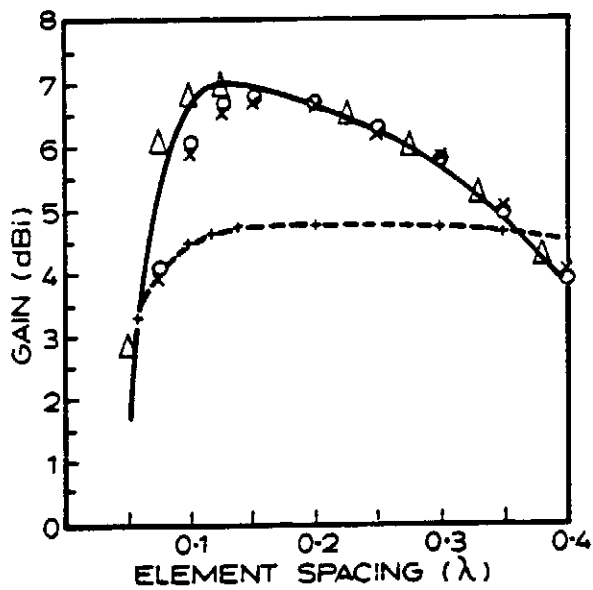


FIG. 4: Computed gain with spacing of the Yagi-Uda array.
 — ref. 20; o MININEC; Δ NEC 2; x ref. 21; -+- ref. 22

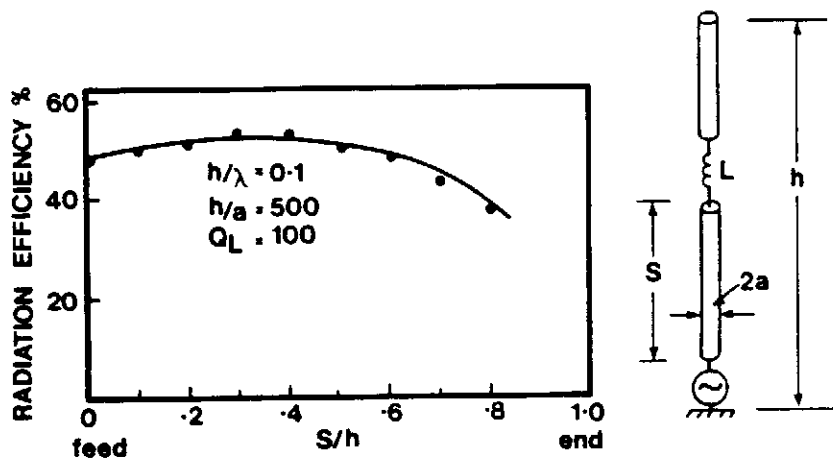


Fig. 5. Radiation efficiency of short loaded monopole;
 — ref. 23, • MININEC

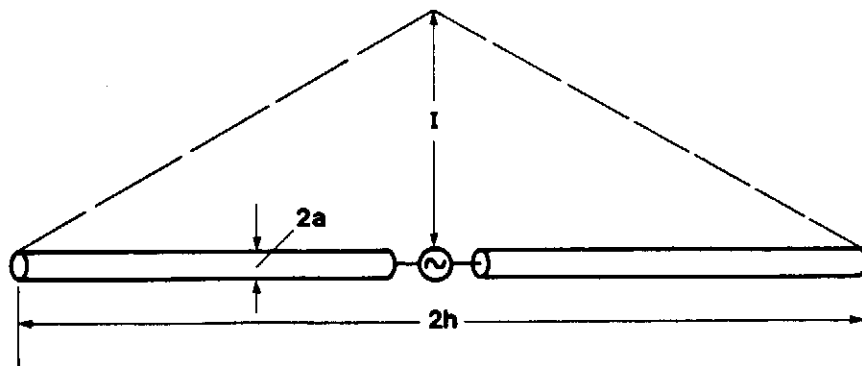


Fig. 6. Thin cylindrical antenna.

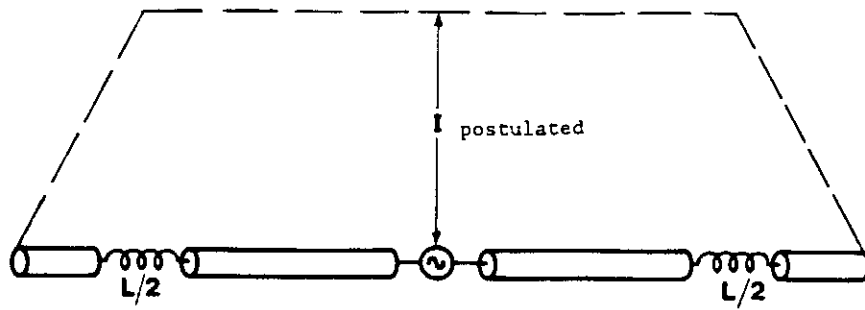


Fig.7. Loaded cylindrical antenna.

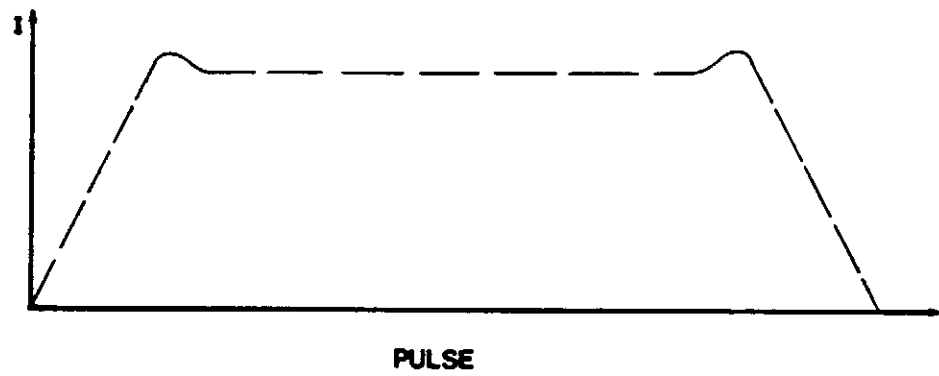


Fig.8. Current distribution: computed.